Assessment of Vulnerability to Erosion in Amazonian Beaches

Remo Pereira , Cesar Mösso Aranda * , Luci Cajueiro

Posted Date: 7 May 2025

doi: 10.20944/preprints202505.0487.v1

Keywords: vulnerability; natural processes; anthropogenic activities; management; Amazonian beaches

 doi:10.20944/preprints202505.0487.v1

Article

Assessment of Vulnerability to Erosion in Amazonian Beaches

Remo Pereira [1], Cesar Aranda [2,*] and Luci Pereira [3]

[1] Universitat Politècnica de Catalunya BarcelonaTech, c/Jordi Girona 1-3, 08034, Barcelona, Spain
[2] Laboratori d'Enginyeria Marítima, Universitat Politècnica de Catalunya BarcelonaTech, c/Jordi Girona 1-3, 08034, Barcelona, Spain.
[3] Institute of Coastal Studies, Universidade Federal do Pará, Alameda Leandro Ribeiro sn, Aldeia, 68600-000, Braganca-Pará, Brazil
* Correspondence: cesar.mosso@upc.edu

Abstract: Erosion represents a significant global threat to coastal zones, especially beaches, which are among the most valuable coastal landforms. This study evaluates the vulnerability to coastal erosion along the Brazilian Amazon coast, focusing on eight recreational beaches. The research is based on an assessment of geological, physical, ecological, and anthropogenic indicators. Some of these indicators were proposed in this study to enhance the evaluation of vulnerability in Amazonian beaches. The analysis reveals that most of the beaches studied are highly vulnerable to erosion due to a combination of natural factors and human activities. The barrier-beach ridge, composed of unconsolidated sediments, exhibits the highest vulnerability, while low cliffs present a moderate level of risk. The study highlights that semi-urban beaches with significant infrastructure development are particularly susceptible to erosion, a problem exacerbated by unplanned land use. Conversely, rural beaches, especially those located in protected areas, show lower vulnerability due to reduced human impact and better conservation of natural ecosystems. Furthermore, the study underscores the effects of extreme climatic events, such as prolonged rainfall and high-energy waves, which can intensify erosion risks. The findings suggest that anthropogenic changes, combined with extreme climate events, significantly influence the dynamics of coastal erosion. This research emphasizes the importance of targeted management strategies that address both natural and human-induced vulnerabilities, aiming to enhance coastal resilience and sustainability for Amazonian beaches.

Keywords: vulnerability; natural processes; anthropogenic activities; management; Amazonian beaches

1. Introduction

Coastal environments form the dynamic interface between land and sea, hosting essential ecosystems, infrastructure, and nearly 40% of the global population [1,2]. These areas are increasingly exposed to natural and anthropogenic pressures, with coastal erosion being a prominent concern [3,4]. Coastal areas, due to their socio-economic and environmental importance, face global challenges associated with erosion, which impacts sandy coastlines across various regions [5,6]. It is estimated that approximately 70% of the world's sandy beaches are experiencing erosion [7], resulting from complex interactions among climatic, oceanographic, and human-induced factors.

Erosive dynamics result from natural processes such as wave action, tides, beach slope, sediment supply, and sea level rise, often intensified by human activities, such as coastal engineering, land-use changes, and uncontrolled urban expansion [8–11]. Consequently, the net loss of sediment along the beach profile, referred to as erosion [12], can lead to significant morphological transformations in these environments [13], threatening local ecosystems [14], infrastructure, and socio-economic

 doi:10.20944/preprints202505.0487.v1

activities, including tourism [15,16]. Storms, among natural forces, are particularly significant, often causing both short- and long-term sediment displacement. In severe cases, these events may lead to permanent alterations in the coastal landscape [17–19]. In addition, unplanned occupation and environmental degradation have contributed to the loss of dunes, mangroves, and built infrastructure [20,21].

To assess coastal vulnerability, various indices have been developed globally [22–24]. These indices make it possible to identify, quantify, and classify coastal environments based on their varying degrees of vulnerability. One of the most widely applied is the Coastal Vulnerability Index (CVI), which was initially introduced by [25]. It integrates physical, geomorphological, and socio-environmental parameters to assess the susceptibility of coastlines to hazards such as sea-level rise, storms, and erosion [26,27]. Based on this, the present study adapts the CVI approach to the unique conditions of Amazonian beaches, which are shaped by powerful physical forces and increasing anthropogenic pressures [28,29].

The objective of this work is to provide a comprehensive assessment of beach vulnerability across distinct climatic contexts along the Amazonian coast, supporting effective management of natural resources and coastal development. Although focused on Pará state, the methods and findings presented here may inform similar efforts in other dynamic coastal settings.

2. Study Area: The Amazon Coast

2.1. Overview of the Amazon Coast

The Brazilian Amazon coast is a vast and dynamic estuarine–marine system shaped by abundant sediment inputs reworked by both fluvial and coastal processes [29–31]. Stretching between 4°N and 4°S, this coastal zone represents about 35% of Brazil's 8,500 km-long shoreline [32]. It includes the immense sediment, nutrient, and organic matter discharge of the Amazon River (Figure 1), which alone contributes nearly 20% of global river discharge (~200,000 $m^3 s^{-1}$ on average) and an estimated 754×10^6 tons of suspended sediments per year [33–35]. Although bedload constitutes only about 1% of the discharge, it accounts for millions of tons annually [36] and sustains extensive sandy beaches and tidal sandflats.

The coastline is dominated by mangroves and comprises various features such as tidal flats, salt marshes, cheniers, beach ridges, deltas, and coastal dunes, making up one of the world's largest mangrove ecosystems [37,38]. Located in a low-latitude region, the Coriolis effect is minimal, making coastal circulation primarily driven by river discharge, prevailing winds, wave action, and meso- to megatidal regimes that create intense tidal currents [29,30].

 doi:10.20944/preprints202505.0487.v1

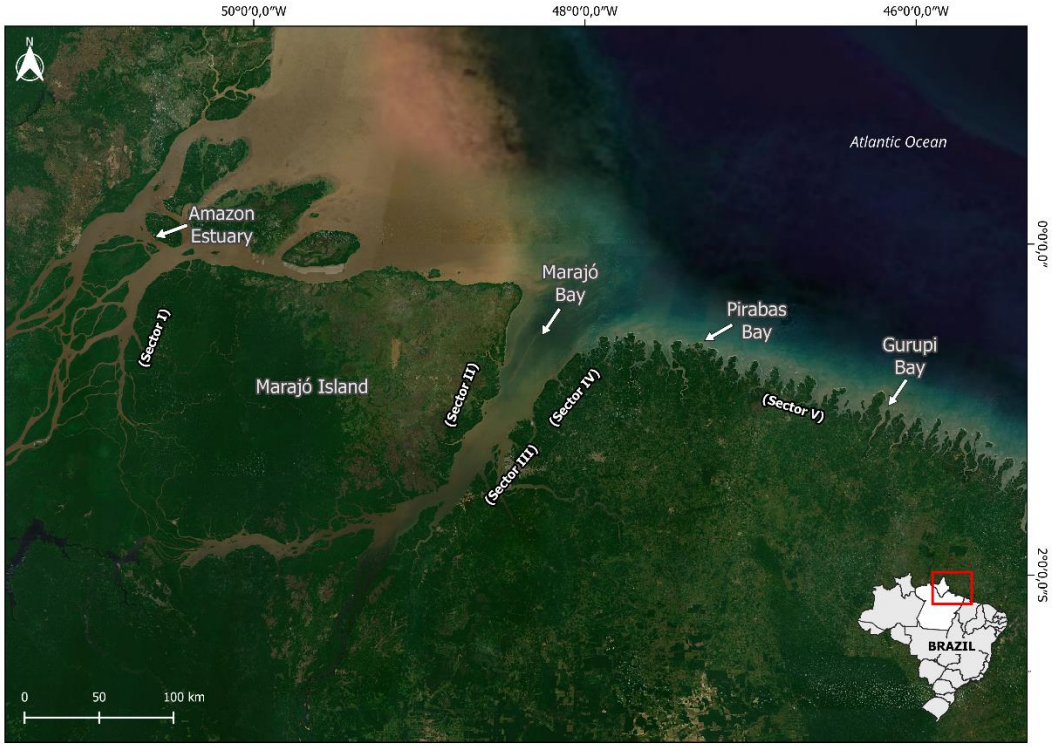

Figure 1. State of Pará highlighting the Amazon and Gurupi estuaries, Marajó Island, Marajó and coastal sectors: Western Marajó (Sector I), the Eastern Marajó (Sector II), the Continental Estuarine (Sector III), the Fluvial Maritime (Sector VI) and the Atlantic Coast of Pará (Sector V) according to [29].

2.2. Geomorphological Setting and Offshore Conditions

From a geomorphological perspective, the Pará coast is divided into two primary zones [39]: (a) the emergent coast, represented by Marajó Island with a relatively straight shoreline, and (b) the submergent coast, extending between Marajó and Gurupi Bays and characterized by a more irregular, dissected landscape with estuaries, islands, and tidal inlets.

This coast is further subdivided based on sedimentary environments and coastal processes. For example, the area between Marajó and Pirabas Bays features a narrow coastal plain and active cliffs formed from Tertiary sediments (Barreiras and Pirabas formations), while the region between Pirabas and Gurupi Bays is distinguished by expansive mangrove areas and sedimentary plains.

Offshore conditions are a critical element in understanding coastal dynamics. Data from NOAA's National Data Buoy Center (Station 41041) indicate that prevailing trade winds—from the northeast and east—drive the generation of waves. During the rainy season (February–May), winds (5.0–14.0 m s^{-1}) produce significant wave heights (H_s) of up to 5.0 m, with predominant directions between 50° and 110° and wave periods of 3 to 19 s. In contrast, during the dry season (September–November), wind speeds and wave heights are generally lower. Figure 2 shows the offshore wind and wave parameters that control the nearshore conditions, setting the stage for coastal processes.

 doi:10.20944/preprints202505.0487.v1

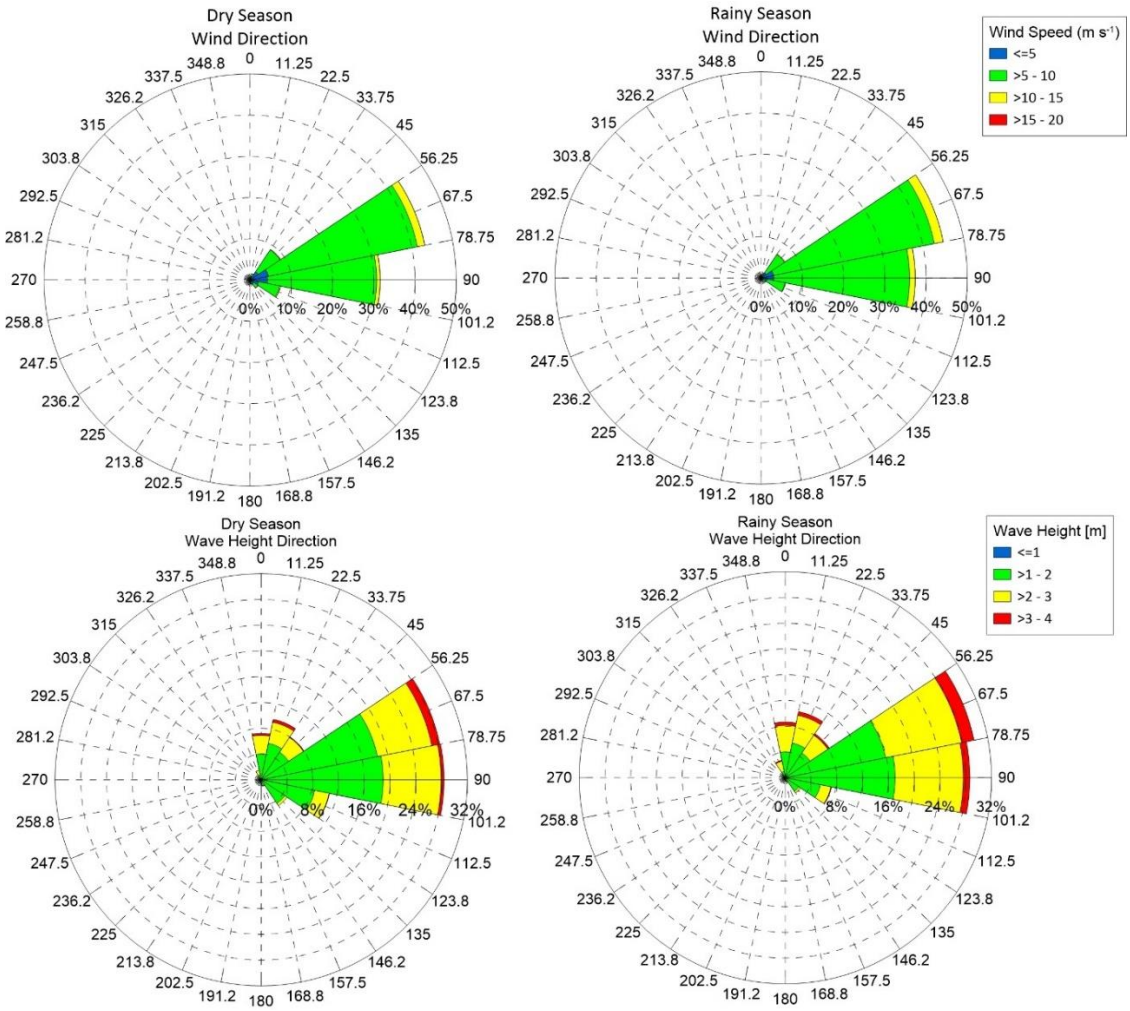

Figure 2. Seasonal pattern of wind (m s^{-1}) and height waves (m) conditions. Source: [40], Buoy Data - 41041.

2.3. Climatic Drivers and Hydrological Dynamics

Rainfall on the Amazon coast is predominantly controlled by the Intertropical Convergence Zone (ITCZ). The region experiences a humid equatorial climate (Köppen Am) with distinct rainy (January–June) and dry (July–December) seasons (Figure 3A). Annual rainfall (Figure 3B) may exceed 2000 mm on the Atlantic coast sector (e.g., Tracuateua station) and 3000 mm within the continental estuarine sector (e.g., Belém station) [41,42].

Interannual climate variability on the Amazon coast is strongly influenced by the Oceanic Niño Index (ONI) for the Niño-3.4 region [40], where El Niño events (ONI ≥ +0.5) reduce rainfall and La Niña events (ONI ≤ -0.5) enhance precipitation. Major El Niño events in 2009–2010 and 2015–2016, as well as La Niña episodes in 2007–2008 and 2010–2011, are clearly reflected in the ONI trends (Figure 4). Additionally, severe droughts—such as those in 2005, 2010, and 2012—have also had notable impacts on regional hydrology, driven in part by elevated sea surface temperatures in the tropical Atlantic.

 doi:10.20944/preprints202505.0487.v1

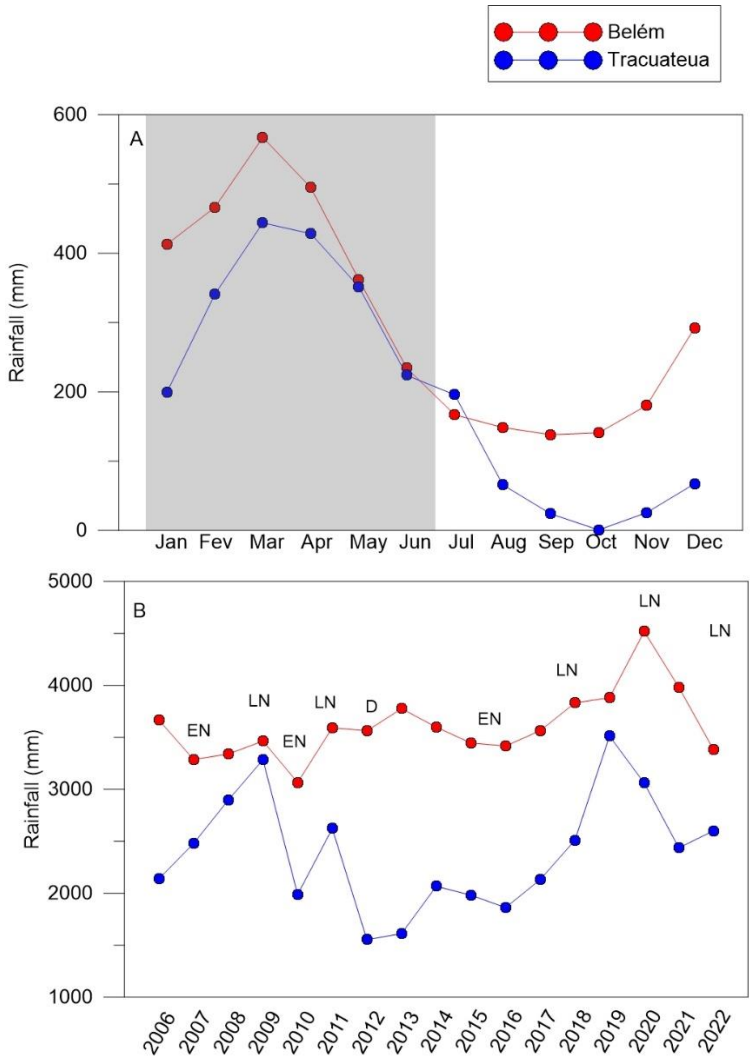

Figure 3. Average monthly rainfall between 2006 and 2022, and annual rainfall (2006-2022) in Belém and Tracuateua. The grey hatching represents the rainy season. EN - *El Niño*, LN - *La Niña* and D - Drought. Source: [43].

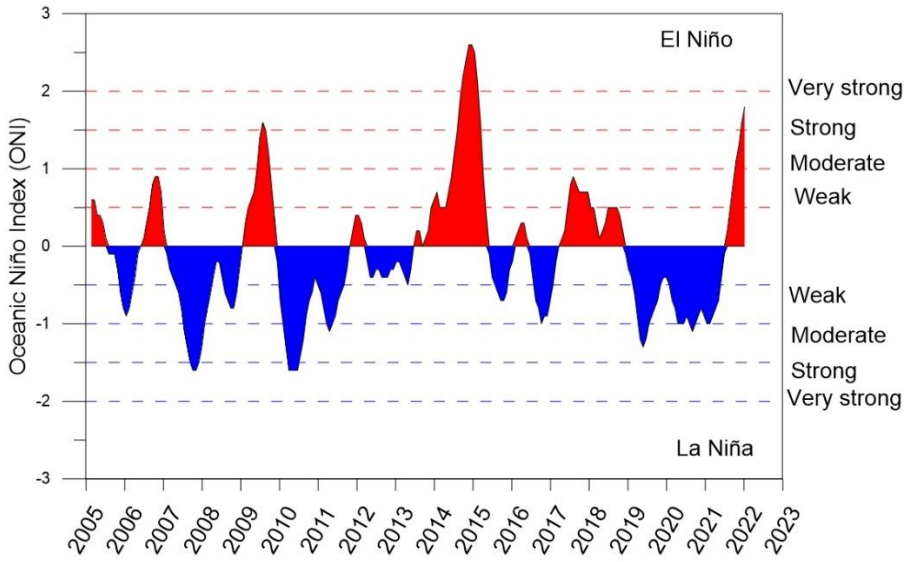

Figure 4. Month Oceanic Niño Index, detaching *El Niño* and *La Niña* levels between 2006 and 2022. Source: [40].

 doi:10.20944/preprints202505.0487.v1

River discharge is closely linked to regional rainfall, with peak flows typically occurring about one month after the highest precipitation periods. Data from the National Water Agency [44] show significant variability between stations, such as the Atlantic Coast Sector (Nova Mocajuba station) and the Continental Estuarine Sector (Guamá station), where Guamá's discharge is approximately 70% higher (Figure 5).

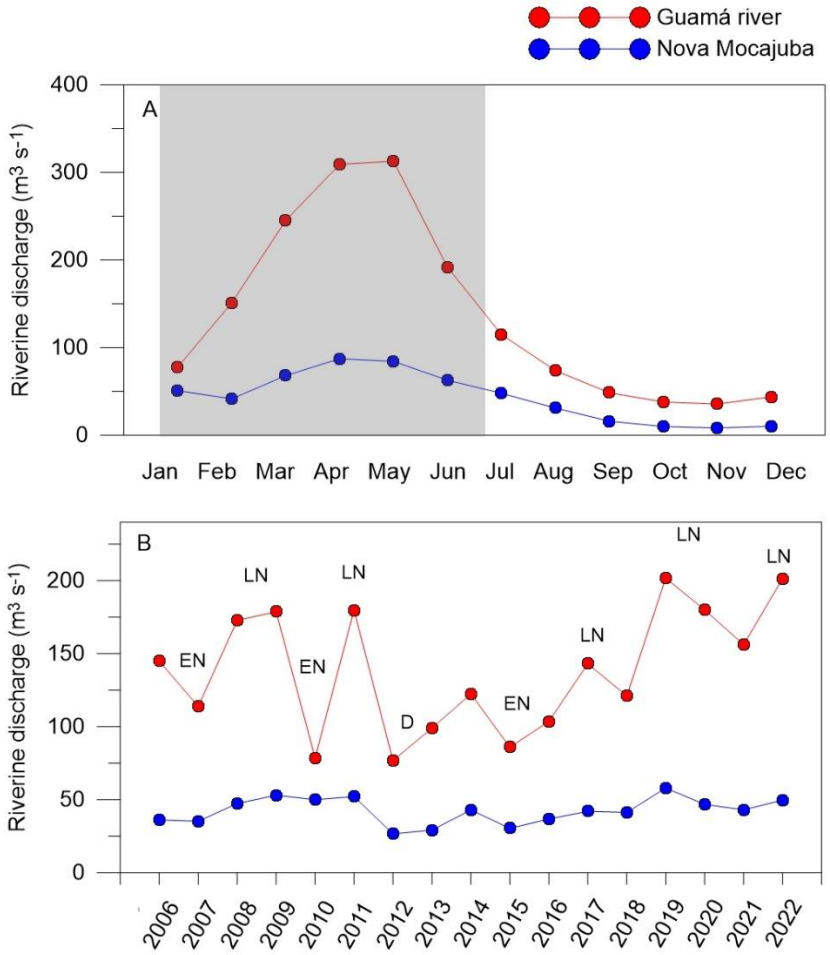

Figure 5. Average monthly riverine discharge between 2006 and 2022, and annual discharge (2006-2022) at the Nova Mocajuba and Guamá stations. The grey hatching represents the rainy season. EN *El Niño*, LN *La Niña* and D Drought. Source: [44].

The wide and shallow Amazonian continental shelf amplifies the tidal range; for instance, tidal amplitudes exceed 4 m in the Atlantic sector (Salinópolis station), but tide attenuation through the Marajó estuary causes a notable reduction in tidal amplitude at Belém and Breves stations (Figure 6).

 doi:10.20944/preprints202505.0487.v1

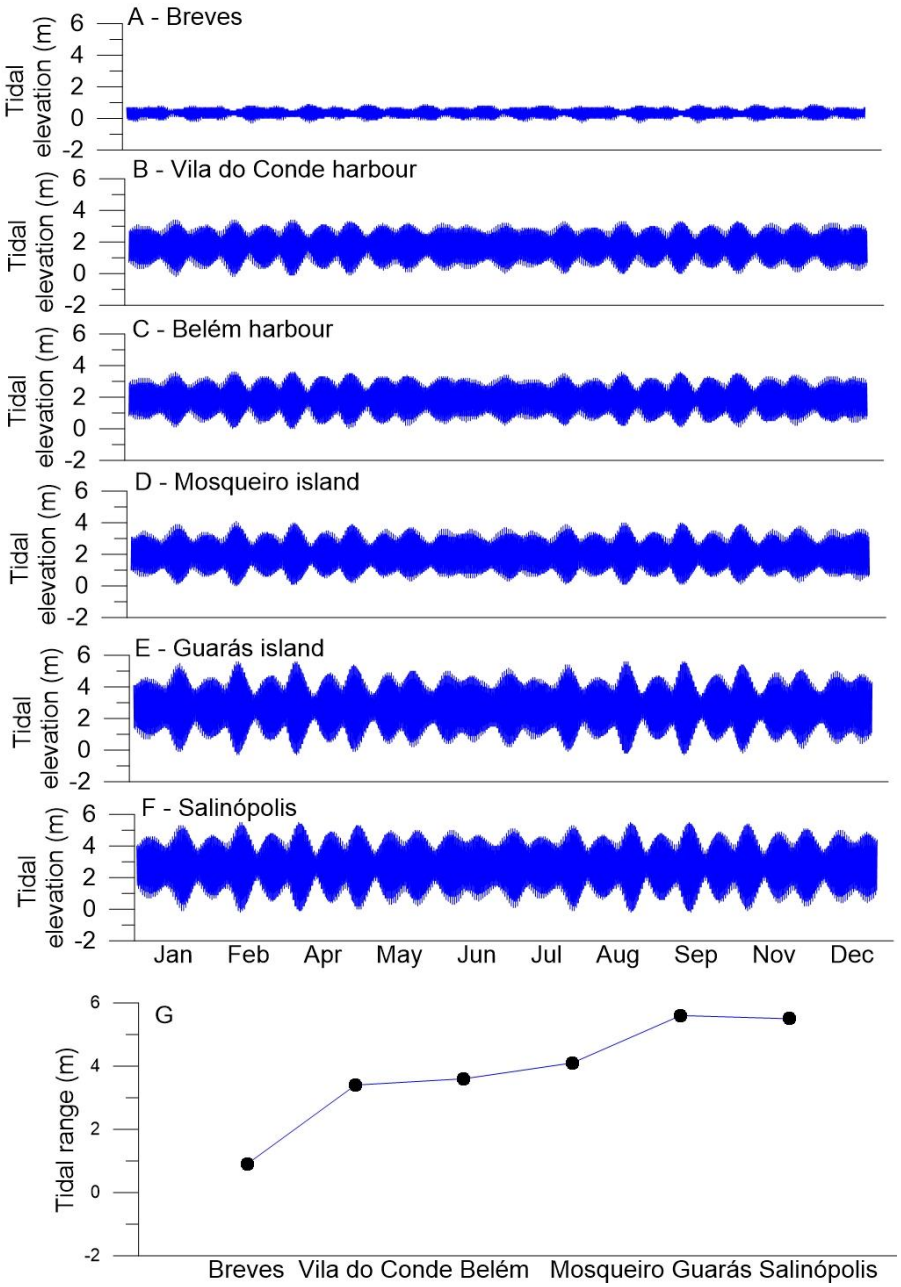

Figure 6. Tidal elevation per month at six stations along the Para coast (A-F), and the maximal range at each station. Source: [45].

2.4. The Study Area and Beach Characteristics

The study area comprises beaches located across four sectors (Figure 7): Eastern Marajó (Pesqueiro and Praia Grande), Continental Estuarine (Murubira), Fluvio-Maritime (Colares, Marudá, and Princesa), and the Atlantic Coast (Atalaia and Ajuruteua).

In the Eastern Marajó sector, Pesqueiro Beach is located in the municipality of Soure. This beach extends approximately 4 km in length and 1 km in width, with a north-south orientation and a straight to convex shoreline. Its gentle slope, segmented by large tidal channels, is influenced by fetch-limited waves from Marajó Bay and strong tidal currents. The fine to very fine sediments contribute to barrier beach formation, while adjacent mangrove and tidal flat systems offer natural shelter. Pesqueiro Beach lies within the Soure Marine Extractive Reserve, supporting traditional artisanal fishing communities. Also in the Eastern Marajó sector, Praia Grande was another beach studied. It features a 1.2 km-long beach with an NNW-SSE orientation, characterized by a narrow, concave sandy strip and steep topography at the base of coastal cliffs. Sediments derived from the Barreiras/Post-Barreiras Group, along with wave action and tidal currents, shape its geomorphology.

 doi:10.20944/preprints202505.0487.v1

In the Continental Estuarine sector, Murubira Beach is situated on Mosqueiro Island along the Pará River. Murubira spans 1.4 km and is about 70 m wide at low tide. The beach is bordered by a series of active and inactive cliffs from the Barreiras Group, with hydrodynamics influenced by tidal ranges of approximately 3.5 m and wave heights reaching 1.5 m.

In the Fluvio-Maritime sector, Colares is a mesotidal beach located on Colares Island. It measures 560 m in length and 400 m in width during low spring tides. Additionally, Marudá Beach, situated at the mouth of the Marapanim estuary, experiences tidal ranges of up to 5 m, spans over 1 km in length, and reaches up to 300 m in width at low tide.

In the Atlantic Coast sector, the studied beaches were Princesa, Atalaia, and Ajuruteua. These insular beaches are surrounded by dunes, estuaries, lagoons, and mangroves. They are characterized by intertidal sandy ridges (200–400 m wide), shaped by macrotidal conditions (tidal ranges >4–6 m) and strong tidal currents (up to 1.5 m s^{-1}). Sandbanks modulate wave energy at low tide, while at high tide, wave heights may exceed 1.5 m. Princesa Beach benefits from additional protection within the Algodoal-Maiandeua Environmental Protection Area, whereas Atalaia and Ajuruteua are near protected areas such as the Caeté-Taperacu Marine Extractive Reserve and the Atalaia Natural Monument.

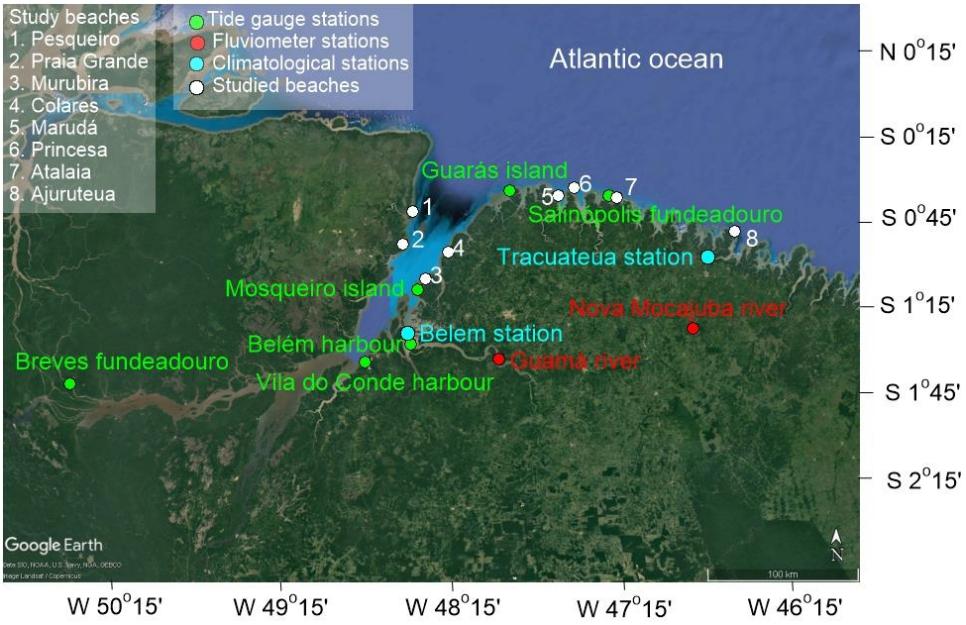

Figure 7. Study area, showing tide gauge, fluviometer and climatological stations, and studied beaches.

3. Methodology

This section introduces the newly proposed Coastal Vulnerability Index (CVI), designed to assess coastal erosion and customized to the specific characteristics of the Amazon coast. The methodology is based on the CVI framework from [46]. The dataset comprises 14 indicators grouped into four categories: Geological (GE), which includes Geomorphology (GM), Beach Slope (BS), Beach Exposure (BE), and Terrain Elevation (TE); Physical (PH), encompassing Wave Climate (WC), Spring Tidal Range (STR), Rainfall Level (RL), and Wave Orientation (WO); Environmental (EN), covering the Conservation Status of Dunes (CD), Conservation Status of Mangrove Forests (CM), and Protected Areas (PA); and Seafront Features (SF), which include Development Level (DL), Territorial Occupation (TO), and Erosion Indicator (EI).

Each CVI component represents a characteristic affecting overall coastal vulnerability, enabling a comprehensive analysis for the eight beaches studied. The indicators were obtained through field campaigns, satellite image analysis, and data from national and international sources (Table 1). The vulnerability scores for each indicator range from 1, indicating Very low vulnerability, to 5, representing Very high vulnerability, as detailed in Table 2. The CVI value was calculated (Eq. 1)

 doi:10.20944/preprints202505.0487.v1

using the arithmetic mean of the indicator values. In this study, the CVI was classified using the same principle applied to the indicators. This standardized scale facilitates the interpretation of the results.

$$CVI = \frac{GM+BS+BE+TE+WC+sTR+RL+WO+CD+CM+PA+DL+TO+EI}{14} \text{ eq.1}$$

Table 1. A summary of the methodology used for the calculation of the CVI.

Sub-indexes	Indicators	Methodology
Geology	Geomorphology	Field campaigns (direct observation), Google Earth satellite images and literature review.
	Beach slope	Field campaigns. Two topographic levelling campaigns were carried out on each beach, from the dunes, backshore area or promenade to the nearshore area (up to 1.5 me deep, relative to the spring low tide level).
	Beach exposure	Field campaigns (direct observation and hydrodynamic measures), Google Earth satellite images and literature review. Hydrodynamics (tidal elevation and significant wave height - H_s) were collected using a mooring mounted on the bottom at a depth of 4.7 m below the MWL, to which wave and tide data loggers (TWR 2050) were attached. Wave sampling was carried out on the basis of 512 samples at a burst rate of 4 Hz, with sampling periods of 10 minutes. Tidal water level data was obtained every 2 seconds and average values were measured every 10 minutes.
	Terrain elevation	Satellite imagery from Google Earth
Physical	Wave climate $H_{s95\%}/H_s$	Field campaigns. Significant wave height-H_s were collected using a bottom-mounted mooring at a depth of 4.7 m below MWL, to which a wave data logger (TWR 2050) was attached. Wave sampling was based on 512 samples at a burst rate of 4 Hz with sampling periods of 10 min duration. Offshore significant wave heights-H_{os} (average height of the highest one-third of all waves measured), periods-T_P (defined as the wave period associated with the most energetic waves in the total wave spectrum at a specific point) and directions-θ were obtained from National Data Buoy Center - NDBC which holds data from NOAA (station 41041)
	Spring Tidal range – sTR	Tidal range was obtained using a bottom-mounted mooring at a depth of 4.7 m below MWL, to which a tide data logger (TWR 2050) was attached. Tidal water level data were obtained every 2s and mean values were measured every 10 min.
	Rainfall level	Monthly precipitation data were provided by the INMET (meteorological stations located at Tracuateua and Belém).
	Wave orientation	The wave direction was obtained from NOAA (station 41041) and the beach orientation was determined using Google Earth and the angle of rotation of the orientation for this shallow angle was obtained using a software program.

 doi:10.20944/preprints202505.0487.v1

Environmental	Conservation status of the dunes	Field campaigns (direct observation)
	Conservation status of the mangrove	Field campaigns (direct observation)
	Protect area	Literature review
Seafront features	Development level	Satellite imagery from Google Earth and field campaign (direct observation)
	Territorial occupation	Satellite imagery from Google Earth and field campaign (direct observation)
	Erosion indicators	Field campaign (direct observation)

Table 2. Ranges of vulnerability scores for the indicators of sub-indexes.

Sub-index	Indicators	Score				
		1-Very low	2-Low	3-Moderate	4-High	5-Very high
Geology (GE)	Geomorphology (GM)	Rocky, cliffed coasts	Medium cliffs and indented coasts	Low cliffs	Estuary and lagoon	Barrier-beach ridge, sandy beaches, muddy or sandy flats bounded by dunes, deltas, mangrove environments
	Beach slope (BS)	>0.12	0.08-0.12	0.04-0.08	0.02-0.04	<0.02
	Beach exposure (BE)	Beaches protected by breakwater or natural barrier, and influenced by high tidal modulation.	Beaches partially protected by natural barrier and with moderate modulation tidal modulation	Beaches partially protected inside the bays, receiving fetch-limited waves	Beaches partially exposed and marked for no modulation of the breaking wave climate	Exposed beaches without protective structures and exhibit no modulation of the breaking wave climate
	Terrain elevation (TE)	> 6 m (estuarine beaches) > 9 m (oceanic beaches)	--	3 to 6 m (estuarine beaches) 6 to 9 m (oceanic beaches)	--	< 3 m (estuarine beaches) and < 6 (oceanic beaches)
Physical (PH)	Wave climate $Hs^2_{95\%}/Hs^2$	<0.65	0.65-0.75	0.75-1.0	1.0-1.5	> 1.5

 doi:10.20944/preprints202505.0487.v1

	Spring Tidal range - sTR	< 1.0 m	1.0-2.0 m	2.0-4.0 m	4.0-6.0 m	> 6.0 m
	Rainfall level	< 300 mm	--	300-700 mm	--	> 700 mm
	Wave orientation	75° -90° 91°-105°	--	60°-74° 106°-120°	--	45°-59° 121°-135°
Environmental (EN)	Conservation status of the dunes	Preserved and vegetated	--	Partially affected: not vegetated dunes, territorial occupation	--	Suppressed
	Conservation status of the mangrove forest	Dense, mature mangroves with no evidence of erosion	--	Partially affected: plants with exposed roots, territorial occupation	--	Little or no trees or leaning trees
	Protect area	Within a protected area	--	Adjacent to a protected area	--	Far from protected area
Seafront features (SF)	Development level	Rural	Semi-urban process	Semi-urban	Urbanization process	Urban
	Territorial occupation	<10%	10-30%	30-50%	50-70%	> 70%
	Erosion indicators*	None	--	1 to 4 indicators	--	>5 indicators

*Indicators: buried vegetation, exposed roots, erosion escarpment, narrowing or absence of backshore, coastal protection engineering structures, state of conservation of dunes, mangroves, cliffs and damage to seafront properties.

3.1. Development of the Coastal Vulnerability Index (CVI)

The geological component includes Geomorphology, which serves as an indicator of the relative erodibility of coastal landforms. For this indicator, vulnerability classification intervals are based on the susceptibility of various relief types, where rocky and cliffed coasts receive the lowest vulnerability scores, while landforms such as beach ridges, sandy beaches, muddy or sandy flats bordered by dunes, deltas, and mangrove environments are assigned the highest scores (Table 2). Another indicator is Beach Slope, which encompasses both the subaerial beach profile (linked to inundation vulnerability) and the submerged slope (associated with erosion potential). Gentle slopes indicate higher vulnerability compared to steeper slopes, as shown in Table 2. This study adopts the ranges provided by [47]. Additionally, Beach Exposure is determined by natural and anthropogenic features, as well as wave-tide interactions (Table 2). The classification system, adapted from [29,48], ranges from sheltered environments that provide physical protection (Very Low vulnerability) to exposed beaches lacking protective structures, with no modulation of the breaking wave climate (Very High vulnerability). The fourth indicator, Terrain Elevation, evaluates the vulnerability of coastal areas to inundation, overwash, and sea-level rise. In this study, the classification criteria were

 doi:10.20944/preprints202505.0487.v1

adapted from [49]. For estuarine beaches, influenced by mesotidal conditions, Very Low vulnerability corresponds to elevations above 6 m, while Very High vulnerability applies to elevations below 3 m. For oceanic beaches, shaped by macrotidal conditions (tidal ranges typically between 5.0 and 6.0 m) and significant wave heights (H_s) up to 1.8 m, Very Low Vulnerability is assigned to elevations above 9 m, and Very High vulnerability to elevations below 6 m. Only three scores, as indicated in Table 2, were used for this indicator to align with those established by [49].

The Physical component encompasses four indicators. The first is Wave Climate, a key factor in coastal sediment balance, particularly during high-energy wave events. According to [47], the ratio between $H_s^2{}_{95\%}$ (wave height exceeded only 5% of the time) and the H_s threshold (which depends on local conditions) defines coastal vulnerability based on erosion potential. When wave heights exceed this threshold, significant erosive impacts can reshape the coastline, damage habitats, and affect infrastructure (Table 2). The second indicator is Spring Tidal Range, which is linked to risks of permanent and episodic flooding. High tidal ranges—especially when combined with strong tidal currents—are associated with increased coastal erosion [50] (Table 2). High Rainfall Levels directly influence the water table and coastal sediment transport. Greater beach saturation enhances sediment movement, increasing erosion (higher vulnerability). Along the Amazon coast, groundwater exfiltration in the upper intertidal zone occurs when cumulative three-month rainfall exceeds 500 mm [51]. The fourth indicator is Wave Direction, which is determined by the angle between beach alignment and prevailing wave directions. Vulnerability is assessed based on criteria outlined in [50], as shown in Table 2.

With respect to the Environmental components, three indicators stand out. The first is the conservation status of dunes, as dunes serve as natural barriers that protect coastal areas and contribute to sediment balance. Adapted from [52], vulnerability classifications range from preserved and vegetated dunes (Very Low vulnerability) to suppressed dunes (Very High vulnerability), as shown in Table 2. The second indicator is the conservation status of mangrove forests, as mangroves act as protective barriers against waves and storms, making them effective indicators of erosion. Vulnerability classifications range from beaches with dense, mature mangroves showing no signs of erosion (Very Low vulnerability) to sparse or absent mangrove trees and leaning vegetation (Very High vulnerability), as shown in Table 2. The last indicator is the presence of protected areas, primarily designated for sustainable use. Vulnerability is ranked from beaches located within protected areas (Very Low vulnerability) to beaches outside and distant from protected areas (Very High vulnerability).

The Seafront features are composed of three indicators. The first is Development Level, which assesses the distribution of populations and settlements to determine the degree of development in an area. This can place pressure on coastal zones and potentially exacerbate coastal erosion. Development levels are categorized into five classifications, as presented in Table 2. The second indicator is Territorial Occupation, which evaluates the percentage of spatial occupation along the seafront. Scores, adapted from [53], are determined based on the percentage of occupation, as outlined in Table 2. The third indicator is Erosion Indicators, which analyze the presence of specific signs of coastal erosion, as shown in Table 2. These indicators include buried vegetation, exposed roots, erosion escarpments, narrowing or absence of the backshore, coastal protection structures, and damage to seafront properties

4. Results

4.1. The Coastal Vulnerability Index-CVI

The Coastal Vulnerability Index (CVI) (Table 3) highlights differences in vulnerability among the studied beaches. The lowest vulnerability scores are observed in rural beaches such as Pesqueiro (CVI = 2.9), Princesa (CVI = 3.2) and Colares (CVI = 3.3). Although geological and physical factors contribute to Moderate to High vulnerability in these areas, their lower overall vulnerability is attributed to the conservation of dune, mangrove, and restinga environments, along with limited development and reduced human impact. Moderate vulnerability scores are assigned to Praia

 doi:10.20944/preprints202505.0487.v1

Grande (CVI = 3.6) and Murubira (CVI = 3.6), primarily due to higher scores in physical factors (such as rainfall levels and wave orientation), environmental aspects (absence of protected areas), and seafront features (erosion indicators). The highest vulnerability scores are recorded for semi-urban beaches, including Marudá (CVI = 4.2), Atalaia (CVI = 4.2), and Ajuruteua (CVI = 4.0). Ajuruteua, although currently a rural beach, is undergoing rapid development and transitioning towards semi-urbanization, increasing its vulnerability. Below is the description of the indicators by sector.

Table 3. Components, Indicators and CVI values per beach.

Components	Indicators	Pesqueiro	Grande	Murubira	Colares	Marudá	Princesa	Atalaia	Ajuruteua
Geology	Geomorphology	5	3	3	3	5	5	5	5
	Beach slope	4	3	3	3	4	5	5	5
	Beach exposure	3	3	3	3	3	1	2	1
	Terrain elevation	3	1	1	3	3	5	5	5
Physical	Wave climate	4	4	4	4	5	5	5	5
	Spring Tidal range	3	3	3	3	5	5	5	5
	Rainfall level	5	5	5	5	5	5	5	5
	Wave orientation	5	5	5	5	5	5	5	5
Environmental	Conservation status of the dunes	1	3	3	1	3	1	3	3
	Conservation status of the mangrove	1	3	3	1	3	1	3	3
	Protect area	1	5	5	5	5	1	3	3
Seafront features	Development level	1	3	3	2	3	1	3	2
	Territorial occupation	2	4	5	4	5	2	5	4
	Erosion indicators	3	5	5	4	5	3	5	5
CVI		2.9	3.6	3.6	3.3	4.2	3.2	4.2	4.0

4.2. Eastern Marajó Island (Sector II)

In this sector, two beaches were analyzed: Pesqueiro and Praia Grande. Pesqueiro Beach exhibited Very High vulnerability in the Geological and Physical components, particularly in the Geomorphology indicator, as it is a barrier beach characterized by a curved spit shaped by local north-south longitudinal sediment transport. Similarly, High vulnerability was observed in the Rainfall level indicator, due to rainfall accumulation exceeding 1500 mm over three months during the rainiest period, and in the Wave orientation indicator. Moreover, High vulnerability was noted in the Beach slope indicator, as the slope typically ranges between 0.02 and 0.04, and in the Wave climate indicator, where the ratio of $H_{s^2 95\%}$ to H_{s^2} falls between 1.0 and 1.5. Conversely, Pesqueiro Beach is situated within a protected area, which results in Low vulnerability for five of the six environmental and seafront feature indicators. It is a rural beach surrounded by well-preserved dunes and mangroves, making it part of the Soure Marine Extractive Reserve. Territorial occupation along the beachfront is less than 30%. The sole exception was the Erosion indicator, which revealed

 doi:10.20944/preprints202505.0487.v1

evidence of buried vegetation, exposed roots, and an erosion escarpment. As a consequence of the erosion issue, the beach area experienced a reduction of 61,202 m² between 2007 and 2021 (Figure 9).

At Praia Grande, six indicators exhibit Moderate vulnerability: two within the Geology component: (i) Geomorphology, as it is a beach with ridges running in a NNW-SSE direction, bordered by cliffs and headlands of the coastal plateau; and (ii) beach slope, which ranges between 0.04 and 0.08. One indicator within the Physical component, the Spring tidal range, reaching 2.0–4.0 m, classifying it as mesotidal. Two indicators within the Environmental component—dunes and mangroves, which are partially affected by nearby construction. Finally, one within the Seafront features component. Very High vulnerability was recorded in the Physical component for Rainfall level and Wave orientation. It is a semi-urban beach located outside protected zones. The Territorial occupation at Praia Grande covers 50–70% of the beachfront, indicating High vulnerability, with Erosion indicators including property damage, cliffs, mangroves, dunes, exposed roots, and a narrow shoreline.

4.3. Continental Estuarine and Fluvio-Maritime (Sectors III and IV)

Four beaches were studied within these sectors: Murubira, Colares, Marudá, and Princesa. Murubira Beach is characterized by active cliffs of the Barreiras Group, indicating Moderate vulnerability. Its Beach slope, ranging between 0.04 and 0.08, is also classified as Moderate vulnerability. About 75% of its terrain has elevations greater than 6 m, corresponding to Very Low vulnerability. Colares Beach features sandy deposits primarily shaped by Wave action, located at the foot of cliffs, resulting in Moderate vulnerability. Its Beach slope, ranging between 0.04 and 0.08, also falls under Moderate vulnerability, with 86% of the coastline at elevations between 3 and 6 m. Marudá Beach consists of sandy ridges, forming banks and channels that create Very High vulnerability (Figure 8). The beach slope, varying from 0.02 to 0.04, indicates High vulnerability, while 100% of the coastline has elevations between 3 and 6 m, marking it as Moderate vulnerability. Princesa Beach is a flat, linear barrier ridge, surrounded by dunes and mangroves, contributing to Very High vulnerability. Its Beach slope, ranging between 0.08 and 0.12, is considered Low vulnerability, but its coastal elevation, measuring less than 6 m, results in Very High vulnerability for this indicator.Among all beaches in these sectors, the $H_s^2{}_{95\%}$ and the H_s^2 ratio exceeded 1.5, only in Princesa beach.

 doi:10.20944/preprints202505.0487.v1

Figure 8. Study beaches showing details of the natural characteristics and development level. The red line represents 2007, the blue line represents 2014, and the green line represents 2021.

In addition, Murubira and Colares exhibit mesotidal conditions, with a Spring tidal range of 3.9 m, indicating Moderate vulnerability, while Marudá and Princesa, with Spring tidal ranges exceeding 4.0 m, fall into the macrotidal category, leading to Very High vulnerability. During the rainiest months, rainfall accumulation surpasses 1500 mm over three months across all beaches, resulting in Very High vulnerability in this regard. The Environmental features further differentiate these beaches. Murubira and Marudá experience significant human impact, with territorial occupation

 doi:10.20944/preprints202505.0487.v1

affecting 70–80% of the coastline, leading to Very High vulnerability. These semi-urban beaches are heavily used for recreational purposes, causing considerable modifications to their original natural conditions, resulting in Moderate vulnerability. Erosion indicators, such as buried vegetation, exposed roots, erosion escarpments, and damage to properties, are prominent in both locations. Colares and Princesa are rural and less developed, which places them in Low and Very Low vulnerability categories, respectively. Colares, in particular, has less than 30% of its coastline occupied by buildings, with well-preserved dunes and native vegetation, denoting Low vulnerability. Princesa Beach, located within the Algodoal/Maiandeua Environmental Protection Area, enforces strict territorial management, ensuring well-conserved dunes and mangroves, contributing to Very Low vulnerability. However, the construction of 30 bars in the intertidal zone adds an element of Low vulnerability to its overall environmental profile. However, at Marudá and Princesa beaches, the surface area decreased by 41,414 m² and 51,910 m², respectively, between 2007 and 2021. In Murubira, the retaining wall helped limit the reduction in surface area to 709 m² during this period (Figure 9).

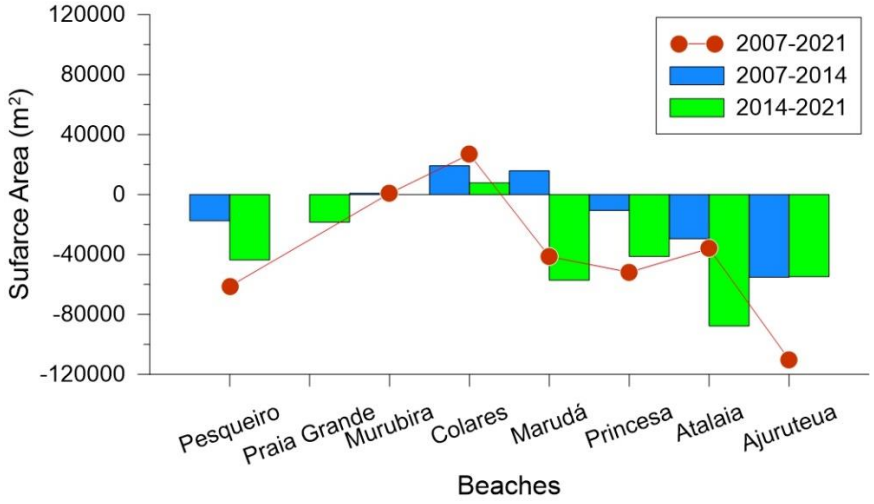

Figure 9. Surface area at different time intervals.

4.4. Atlantic Coast (Sector V)

The two beaches analyzed in this sector, Ajuruteua and Atalaia, are geomorphologically classified as highly vulnerable due to their barrier beach ridge characteristics (Figure 8). Both beaches are flat, linear, elongated landforms, bordered by tidal deltas, dunes, and mangrove areas, contributing to their Very High vulnerability. Additionally, the beach slope is absent in both Ajuruteua and Atalaia, further emphasizing their Very High vulnerability. During low tide, semi-submerged sandbanks offer protection to both beaches. Ajuruteua provides better protection during low tide, with wave heights (H_s values) ranging from 0.1 to 0.4 m, while Atalaia offers less protection, with H_s values between 0.5 and 0.8 m. The seafront terrain elevation ranges from 3 to 9 m, yet inhabited areas reveal that 52% of Ajuruteua's coastline and 77% of Atalaia's coastline feature elevations below 6 m, placing both beaches in the Very High vulnerability category.

The physical indicators further reflect their susceptibility to erosion. The $H_s^2{}_{95\%}$ and the H_s^2 threshold ratio exceeded 1.5, indicating Very High vulnerability. This ratio signifies that wave heights exceeded 5% of the time are greater than 2.5 m, demonstrating significant erosion potential. Additionally, the spring tidal range (sTR) for both beaches varies between 5 and 6 m, representing high vulnerability. Rainfall accumulation during the wettest months surpasses 1500 mm over three months, confirming very high vulnerability in this regard.

In addition, Ajuruteua is adjacent to the Caeté-Taperaçu Marine Extractive Reserve, established in 2005, while Atalaia is adjacent to the Atalaia Natural Monument, created in 2018. Both beaches feature numerous wooden structures built on stilts within the intertidal zone, dunes, and mangrove areas. Territorial occupation affects 50–70% of Ajuruteua's coastline, resulting in High vulnerability,

 doi:10.20944/preprints202505.0487.v1

while Atalaia's territorial occupation exceeds 70%, placing it in the Very High vulnerability category. Ajuruteua retains rural characteristics but is transitioning into semi-urbanization, presenting Low vulnerability. Several houses, bars, and restaurants line its seafront, whereas Atalaia Beach exhibits significant semi-urbanization, with extensive construction of bars, hotels, and houses, contributing to moderate vulnerability. With respect to erosion, both beaches have experienced substantial erosion over the decades, leading to the partial or complete destruction of buildings, infrastructure, dunes, and mangroves. Equinoctial spring tides exacerbate erosion events, resulting in the loss of street lighting, bars, restaurants, and inns. At Atalaia, wooden structures are frequently relocated to dunes during periods of severe erosion, while Ajuruteua has implemented structural engineering solutions to protect its buildings. However, Ajuruteua's surface area has decreased by 110,046 m² betweem 2007-2021 (Figure 9). Common erosion indicators at both beaches include buried vegetation, exposed roots, escarpments, concentrations of heavy minerals, coastal protection structures, and damage to seafront properties.

5. Discussion

5.1. Geological Indicators

Coastal erosion vulnerability is assessed through indicators that reflect susceptibility to high-energy events [27,47,54]. In this study, the Coastal Vulnerability Index (CVI) incorporates geological, physical, environmental, and seafront indicators. Geomorphology was classified based on the relative resilience of coastal landforms [8,55,56]. Two types of coastal relief were identified: (i) barrier beach ridges -composed of unconsolidated sediments and highly vulnerable (score 5)- found in Pesqueiro, Marudá, Princesa, Atalaia, and Ajuruteua; and (ii) low cliffs, moderately vulnerable, in Praia Grande, Murubira, and Colares. Beach slope, a key erosion predictor, shows that gentler slopes are more prone to erosion [49,57]. Protection levels—natural or artificial—also modulate exposure: (i) Estuarine beaches within bays (e.g., Marajó Bay) are Moderate vulnerability due to limited fetch; (ii) Partially protected beaches (e.g., with sandbanks or tidal bars) show Very Low vulnerability; (iii) Less sheltered beaches, like Atalaia, exhibit Low vulnerability [29]. Elevation proved to be crucial: beaches below 6 m are highly vulnerable, 6–9 m moderately so, and above 9 m have low vulnerability (modified from [48]). High vulnerability coincides with barrier beach ridges, while low cliffs correspond to lower vulnerability.

5.2. Physical Indicators

Tidal attenuation reduces tidal elevation by ~35% in Marajó Bay compared to the Atlantic coast. Thus, macrotidal beaches (Atlantic) are more vulnerable due to stronger currents and flooding risk, contrary to previous classifications [46,58]. On the Amazon coast, macrotides and moderate waves drive intense erosion, particularly during equinoctial spring tides [28,51]. Offshore waves (3–4 m) attenuate nearshore (1–2 m), with sandbanks buffering wave energy at low tide. However, high tide exposes the shoreline to wave impact, making it the critical period for erosion. Storm-induced vulnerability is classified as very high (CVI > 1.5) due to significant H_s values (1.5–1.8 m). Wave incidence angles ($\theta > 70°$) increase exposure [56,59]. Rainfall also contributes: heavy seasonal rains saturate beaches, enhancing offshore sediment transport and erosion [60]. All beaches showed High vulnerability due to intense rainfall.

5.3. Environmental Indicators

Dune fields and coastal vegetation—such as mangroves and restinga—serve as critical natural barriers. They not only mitigate the direct impact of waves and storms on the coast but also play a central role in maintaining the sediment balance by acting as both buffers and sources of sediment for neighboring areas. In the study area, rural beaches with well-preserved dune systems and mangroves (e.g., Pesqueiro, Colares, and Princesa) demonstrated Low vulnerability to erosive processes, highlighting the protective function of these natural elements. In addition, the existence of protected areas, where local regulations restrict unplanned urban expansion and promote coastal

 doi:10.20944/preprints202505.0487.v1

ecosystem preservation [61–63], reinforces the resilience of these coastal zones. Such areas facilitate the implementation of sustainable management strategies and effective land-use regulations, which are essential for maintaining the natural stability of the coastline. In contrast, unregulated development and disorganized territorial occupation alter sedimentary processes and significantly increase erosion risk [64,65]. This unsustainable development undermines the natural recovery capability of coastal ecosystems, making them more vulnerable to extreme events.

5.4. Seafront Features

In terms of seafront features, semi-urban beaches like Murubira, Atalaia, and Marudá are characterized by a higher concentration of facilities and services—including restaurants, bars, private residences, inns, and hotels—which intensifies the pressure on these coastal zones. In areas with high territorial occupation (e.g., Praia Grande, Murubira, Marudá, Atalaia, and Ajuruteua), increased anthropogenic activity often exacerbates the natural processes of erosion. The presence of infrastructure limits the natural adaptability of the coast, often aggravating erosion by altering natural sediment dynamics.

When erosion intensifies, it frequently results in significant structural impacts: wooden buildings might be relocated to avoid total loss of utility, whereas concrete constructions could suffer partial or complete failure. Visible signs of erosion include deteriorating structures, exposed tree roots, and the tilting or collapse of trees, which are indicators of severe substrate instability. Although some coastal protection structures have been installed in locations such as Atalaia, Ajuruteua, and Murubira, these interventions are typically limited in scope and sometimes insufficient to counteract the severe impact of extreme weather events.

Furthermore, climatic phenomena like El Niño and La Niña amplify these challenges by causing alternating periods of drought and intense rainfall. These events not only increase rainfall intensity and wave energy during strong wind conditions but also elevate groundwater levels, further destabilizing the coastal landscape. The compounded influence of natural forces and human activities underscores the importance of comprehensive vulnerability assessments. Such integrated analyses are crucial for devising sustainable coastal management strategies and for planning interventions aimed at mitigating the adverse effects of coastal erosion.

6. Summary and Conclusions

This study evaluated the erosion vulnerability of eight beaches along the Pará coast (Amazonian coast, Brazil) by integrating geomorphological characteristics, coastal physical processes, patterns of territorial occupation, ecosystem conservation, and erosion indicators. The analysis revealed a vulnerability spectrum ranging from low to high across the study area. Natural factors play a crucial role, as the inherent geology and physical processes largely drive high vulnerability in most of the beaches. Anthropogenic impacts further exacerbate vulnerability, with unplanned territorial occupation significantly affecting semi-urban beaches (e.g., Atalaia) or in semi-urban process (e.g., Ajuruteua) with higher development. In contrast, rural beaches, particularly those within protected areas, demonstrated lower vulnerability due to reduced human interference and better preservation of natural protective features. However, evidence of erosion was recorded in Princesa and Pesqueiro beaches. The presence of promade on the semi-urban beaches of Marudá, Murubira, and Colares prevented them from experiencing significant variations in the coastline; Extreme meteorological events, including prolonged rainfall and intensified wave activity, also contribute to erosion, temporarily heightening erosive processes and disrupting coastal equilibrium. These episodic events can accelerate erosion, posing additional threats to coastal stability. The findings highlight the necessity of integrating comprehensive vulnerability assessments into coastal management practices. They provide critical support for the development and implementation of mitigation strategies to reduce erosion impacts on both estuarine and oceanic beaches, regardless of urbanization levels. Overall, the study offers valuable insights for the sustainable management of natural resources and

 doi:10.20944/preprints202505.0487.v1

infrastructure preservation along the Amazonian coast, emphasizing the need for proactive and adaptive management strategies in response to both natural and human-induced challenges.

Author Contributions: Conceptualization, Pereira RLMC, Pereira LCC and Aranda CM; methodology, RLMC, Pereira LCC and Aranda CM; validation, RLMC, Pereira LCC and Aranda CM; formal analysis, RLMC, Pereira LCC and Aranda CM; investigation, RLMC and Pereira LCC; resources, RLMC, Pereira LCC and Aranda CM; data curation, RLMC, Pereira LCC and Aranda CM; writing—original draft preparation, RLMC, Pereira LCC and Aranda CM; supervision, RLMC and Aranda CM; funding acquisition, Pereira LCC. All authors have read and agreed to the published version of the manuscript.

Funding: This research was funded by Brazilian National Council for Scientific and Technological Development - CNPq (483913/2012-0, 431295/2016-6, 314037/ 2021–7).

Data Availability Statement: Data will be available on request.

Acknowledgments: This study was financed by the Brazilian National Council for Scientific and Technological Development (CNPq) through a Universal Project (483913/2012-0, 431295/2016-6). The authors Pereira LCC (314037/2021–7) would also like to thank CNPq for its research grants.

Conflicts of Interest: The authors declare no conflicts of interest.

References

1. Martinez, M.L., Intralawan, A., Vázquez, G., Pérez-Maqueo, O., Sutton, P., Landgrave, R. The coasts of our world: Ecological, economic and social importance. *Ecol Econ* **2007**, *63*(2-3), 254-272. https://doi.org/10.1016/j.ecolecon.2006.10.022.
2. Barbier, E.B., Hacker, S.D., Kennedy, C., Koch, E.W., Stier, A.C., Silliman, B.R. The value of estuarine and coastal ecosystem services. *Ecol Monogr* **2011**, *81*(2), 169-193. https://doi.org/10.1890/10-1510.1
3. Prasad, D. H., Kumar, N.D. Coastal erosion studies—a review. *Int J Geosci* **2014**, *5* (3). doi:10.4236/ijg.2014.53033
4. Vousdoukas, M.I., Ranasinghe, R., Mentaschi, L., Plomaritis, T.A., Athanasiou, P., Luijendijk, A., Feyen, L. Sandy coastlines under threat of erosion. *Nat Clim Chang* **2020**, *10*(3), 260-263. https://doi.org/10.1038/s41558-020-0697
5. Pranzini, E., Williams, A.T. *Coastal erosion and protection in Europe*. London, UK: Routledge. 2013. 457p.
6. Mentaschi, L., Vousdoukas, M.I., Pekel, J.F., Voukouvalas, E., Feyen, L. Global long-term observations of coastal erosion and accretion. *Sci Rep* **2018**, *8*(1), 12876. https://doi.org/10.1038/s41598-018-30904-w
7. Davis, R. A. JR., FitzGerald, D. M. *Beaches and coasts*. (1st ed.). Blackwell science Ltd, 419. 2004. doi:10.1002/9781119334491
8. Karymbalis, E., Chalkias, C., Chalkias, G., Grigoropoulou, E., Manthos, G., Ferentinou, M. Assessment of the sensitivity of the southern coast of the Gulf of Corinth (Peloponnese, Greece) to sea-level rise. *Cent Eur Geol* **2012**, 4(4), 561-577. doi:10.2478/s13533-012-0101-3
9. Temmerman, S., Meire, P., Bouma, T.J., Herman, P.M., Ysebaert, T., Vriend, H.J. Ecosystem-based coastal defence in the face of global change. *Nature* **2013**, *504*(7478), 79-83. doi: 10.1038/nature12859.
10. Biel, R.G., Hacker, S.D., Ruggiero, P., Cohn, N., Seabloom, E.W. Coastal protection and conservation on sandy beaches and dunes: context-dependent tradeoffs in ecosystem service supply. *Ecosphere* **2017**, *8*(4), https://doi.org/10.1002/ecs2.1791.
11. McLachlan, A., Defeo, O., Short, A.D. Characterising sandy beaches into major types and states: Implications for ecologists and managers. *Estuar Coast Shelf Sci* **2018**, *215*, 152–160. doi: 10.1016/j.ecss.2018.09.027.
12. Antolinez, J.A.A., Méndez, F.J., Camus, P., Vitousek, S., González, E.M., Ruggiero, P., Barnard, P. A multiscale climate emulator for long-term morphodynamics (MUSCLE-morpho). *J Geophys Res Oceans* **2016**, *121*(1), 775-791. https://doi.org/10.1002/2015JC011107
13. Harley, M.D., Masselink, G., Alegría-Arzaburu, R.A., Valiente, N.G., Scott, T. Single extreme storm sequence can offset decades of shoreline retreat projected to result from sea-level rise. *Commun Earth Environ* **2022**, *3*(1), 112. https://doi.org/10.1038/s43247-022-00437-2

 doi:10.20944/preprints202505.0487.v1

14. Thakur, S., Mondal, I., Bar, S., Nandi, S., Ghosh, P.B., Das, P., De, T.K. Shoreline changes and its impact on the mangrove ecosystems of some islands of Indian Sundarbans, North-East coast of India. *J Clean Prod* **2021**, *284*, 124764. https://doi.org/10.1016/j.jclepro.2020.124764
15. Phillips, M.R., Jones, A.L., Erosion and tourism infrastructure in the coastal zone: Problems, consequences and management. *Tour Manag* **2006**, *27*(3), 517-524. https://doi.org/10.1016/j.tourman.2005.10.019
16. Roig-Munar, F.X., Mir-Gual, M., Rodríguez-Perea, A., Pons, G.X., Martín-Prieto, J.A., Gelabert, B., Blázquez-Salom, M. Beaches of Ibiza and Formentera (Balearic Islands): a classification based on their environmental features, tourism use and management. *J Coast Res* **2013**, *65*, 1850-1855. https://doi.org/10.2112/SI65-313.1
17. Splinter, K.D., Carley, J.T., Golshani, A., Tomlinson, R. A relationship to describe the cumulative impact of storm clusters on beach erosion. **Coast Eng** *2014*, *83*, 49-55. https://doi.org/10.1016/j.coastaleng.2013.10.001
18. Harley, M.D., Turner, I.L., Kinsela, M.A., Middleton, J.H., Mumford, P.J., Splinter, K.D., Short, A.D. Extreme coastal erosion enhanced by anomalous extratropical storm wave direction. *Sci Rep* **2017**, *7*(1), 6033. https://doi.org/10.1038/s41598-017-05792-1
19. Ciavola, P., Coco, G. *Coastal storms: processes and impacts*. John Wiley & Sons. 2004. doi:10.1002/9781118937099
20. Pereira, L.C.C., Guimarães, D.O., Ribeiro, M.J.S., Costa, R.M., Souza-Filho, P.W.M. Use and occupation in Bragança littoral, Brazilian Amazon. *J Coast Res* **2007**, *SI 50*, 1116–1120.
21. Pereira, L.C.C., Sousa-Felix, R.C., Costa, R.M., Jimenez, J.A. Challenges of the recreational use of Amazon beaches. *Ocean Coast Manag* **2018**, *165*, 52-62. https://doi.org/10.1016/j.ocecoaman.2018.08.012
22. Sharples, C.H.R.I.S. Indicative mapping of Tasmanian coastal geomorphic vulnerability to sea-level rise using GIS line map of coastal geomorphic attributes. Consultant Report to Department of Primary Industries & Water, Tasmania. 2016
23. Narra, P., Coelho, C., Sancho, F., Escudero, M., Silva, R. Coastal hazard assessments for sandy coasts: appraisal of five methodologies. *J Coast Res* **2019**, 35(3), 574-589. https://doi.org/10.2112/JCOASTRES-D-18-00083.1
24. Rodríguez-Rosales, B., Abreu, D., Ortiz, R., Becerra, J., Cepero-Acán, A.E., Vázquez, M.A., Ortiz, P. Risk and vulnerability assessment in coastal environments applied to heritage buildings in Havana (Cuba) and Cadiz (Spain). *Sci Total Environ* **2021**, *750*, 141617. https://doi.org/10.1016/j.scitotenv.2020.141617
25. Gornitz V.M. Vulnerability of the East Coast USA to future sea level rise. *J Coast Res 1990*, **9**, 201-237.
26. Kumar, A., Kunte, P.D. Coastal vulnerability assessment for Chennai, east coast of India using geospatial techniques. *Nat Hazards (Dordr)* **2012**, *64*, 853-872. https://doi.org/10.1007/s11069-012-0276-4
27. Pantusa, D., D'Alessandro, F., Riefolo, L., Principato, F., Tomasicchio, G.R. Application of a coastal vulnerability index. A case study along the Apulian Coastline, Italy. **Water** *2018*, *10*(9), 1218. https://doi.org/10.3390/w10091218
28. Pereira, L.C.C., Vila-Concejo, A., Costa, R.M., Short, A.D. Managing physical and anthropogenic hazards on macrotidal Amazon beaches. *Ocean Coast Manag* **2014**, *96*, 149-162. https://doi.org/10.1016/j.ocecoaman.2014.05.008
29. Pereira, L.C.C., Vila-Concejo, A., Short, A.D. *Coastal Morphodynamic Processes on the Macro-Tidal Beaches of Pará State Under Tidally Modulated Wave Conditions.* In: Short, A., Klein, A. (eds) Brazilian Beach Systems. Coastal Research Library, vol 17. Springer Cham. 2016. https://doi.org/10.1007/978-3-319-30394-9_4
30. Anthony, J.E., Gardel, A., Proisy, C., Fromard, F., Gensac, E., Peron, C., Walcker, R., Lesourd, S. The role of fluvial sediment supply and river-mouth hydrology in the dynamics of the muddy Amazon-dominated Amapá-Guianas coast South America: a three-point research agenda. *J S Am Earth Sci* **2013**, *44*, 18–24. doi:10.1016/J.JSAMES.2012.06.005
31. Anthony, J.E., Gardel, A., Gratiot, N. Fluvial sediment supply, mud banks, cheniers and the morphodynamics of the coast of South America between the Amazon and Orinoco river mouths. Geological Society, London, Special Publications 388.1: 533-560. 2014. https://doi.org/10.1144/sp388.8
32. Isaac, V.J., Barthem, R.B. *Os Recursos pesqueiros da Amazônia brasileira*. PR-MCT/CNPq Museu Paraense Emílio Goeldi. 1995.

 doi:10.20944/preprints202505.0487.v1

33. Meade, R.H., Rayol, J.M., Conceicão, S.C., Natividade, J.R. Backwater effects in the Amazon River basin of Brazil. *Environ Geol Water Sci* **1991**, *18*(2), 105-114. https://doi.org/10.1007/BF01704664
34. Moura, R.L., Amado-Filho, G.M., Moraes, F.C., Brasileiro, P.S., Salomon, P.S., Mahiques, M.M., Thompson, F.L. An extensive reef system at the Amazon River mouth. *Sci Adv* **2016**, *2*(4), e1501252. Doi: 10.1126/sciadv.1501252
35. Anthony, J.E, Gardel, A., Gratiot, N., Proisy, C, Allison, M.A., Dolique, F., Fromard, F. The Amazon-influenced muddy coast of South America: a review of mud-bank–shoreline interactions. *Earth Sci Rev* **2010**, *103*(3-4):99–121. https://doi.org/10.1016/j.earscirev.2010.09.008.
36. [36].Dunne, T., Mertes, L.A.K., Meade, R., Richey, J.E., Forsberg, B.R. Exchanges of sediment between the floodplain and channel of the Amazon in Brazil. *Geol Soc Am Bull* **1998**, *110*(4):450–467. https://doi.org/10.1130/0016-7606(1998)110<0450:EOSBTF>2.3.CO;2
37. Kjerfve, B., Lacerda, L.D. *Mangroves of Brazil*. In: Lacerda LD (ed) Conservation and sustainable utilization of mangrove forests in Latin America and Africa regions. International Society for Mangrove Ecosystems, Okinawa, 1993. pp 245–272.
38. Souza-Filho, P.W.M., Morais Tozzi, H. A., El-Robrini, M. Geomorphology, land-use and environmental hazards in Ajuruteua macrotidal sandy beach, northern Brazil. *J Coast Res* **2003**, 580-589. https://www.jstor.org/stable/40928810
39. Franzinelli, E. *Evolution of the geomorphology of the coast of the State of Pará Brazil*. In: Prost MT (ed) Évolution des littoraux de Guyane et de la Zone Caraïbe Méridionale pendant le Quaternaire. ORSTOM, Paris, 1992. pp 203–230.
40. National Oceanic and Atmospheric Administration-NOAA, 2024. Buoy Data - 41041 Middle Atlantic ncei.noaa.gov/access/marine-environmental-buoy-database/41041.html
41. Figueroa, S.N., Nobre, C.A. Precipitations distribution over central and western tropical South America. *Climanálise* **1990**, *5*, 36–45
42. Marengo, J.A. Interannual variability of deep convection over the tropical South American sector as deduced from ISCCP C2 data. *Int J Climatol* **1995**, *15*(9), 995-1010.
43. Agência Bacional de Águas - ANA., 2024. https://www.gov.br/ana/pt-br
44. Instituto Nacional de Meteorologia – INMET, 2024. Monitoramento das estações automáticas. http://www.inmet.gov.br/sonabra/maps/automaticas.php
45. Centro de Hidrografia da Marinha - CHM, 2024. Tábuas de maré. www.marinha.mil.br/chm/dados-do-segnav/dados-de-mare-mapa
46. Thieler, E.R., Hammar-Klose, E.S. National assessment of coastal vulnerability to sea-level rise: preliminary results for the US Atlantic coast (No. 99-593). US Geological survey. 1999.
47. López Royo, M., Ranasinghe, R., Jiménez, J.A. A rapid, low-cost approach to coastal vulnerability assessment at a national level. *J Coast Res* **2016**, *32*(4), 932-945.
48. Mangor, K., Drønen, N.K., Kærgaard, K.H., Kristensen, S. E. Shoreline management guidelines. 2004.
49. Bush, D.M., Neal, W.J., Young, R.S., Pilkey, O.H. Utilization of geoindicators for rapid assessment of coastal-hazard risk and mitigation. *Ocean Coast Manag* **1999**., *42*(8), 647-670. https://doi.org/10.1016/S0964-5691(99)00027-7.
50. Tragaki, A., Gallousi, C., Karymbalis, E. Coastal hazard vulnerability assessment based on geomorphic, oceanographic and demographic parameters: The case of the Peloponnese (Southern Greece). *Land* **2018**, *7*(2), 56. https://doi.org/10.3390/land7020056
51. Pereira, L., Concejo, A.V., Trindade, W. Tidal modulation. In Sandy Beach Morphodynamics. Elsevier. 2020, pp. 87-101 https://doi.org/10.1016/B978-0-08-102927-5.00005-9.
52. Sousa, P.H.G.O. Vulnerabilidade à erosão costeira no litoral de São Paulo: Interação entre processos costeiros e atividades antrópicas (PhD dissertation) São Paulo: Universidade de São Paulo, Instituto Oceanográfico. 2013.
53. Silva, I.R., Pereira, L.C.C., Trindade, W.N., Magalhaes, A., Costa, R.M. Natural and anthropogenic processes on the recreational activities in urban Amazon beaches. *Ocean Coast Manag* **2013**, *76*, 75-84. https://doi.org/10.1016/j.ocecoaman.2012.12.016

 doi:10.20944/preprints202505.0487.v1

54. Alexandrakis, G., Poulos, S. An holistic approach to beach erosion vulnerability assessment. *Sci Rep* **2014**, *4*, 6078. https://doi.org/10.1038/srep06078
55. Nageswara Rao, K., Subraelu, P., Venkateswara Rao, T., Hema Malini, B., Ratheesh, R., Bhattacharya, S., Ajai. Sea-level rise and coastal vulnerability: an assessment of Andhra Pradesh coast, India through remote sensing and GIS. *J Coast Conserv* **2008**., *12*, 195-207. https://doi.org/10.1007/s11852-009-0042-2
56. Andrade, T.S., Sousa, P.H.G.O., Siegle, E. Vulnerability to beach erosion based on a coastal processes approach. *Appl Geogr* **2019**, *102*, 12-19. https://doi.org/10.1016/j.apgeog.2018.11.003.
57. Bozzeda, F., Ortega, L., Costa, L. L., Fanini, L., Barboza, C. A., McLachlan, A., Defeo, O. Global patterns in sandy beach erosion: unraveling the roles of anthropogenic, climatic and morphodynamic factors. *Front Mar Sci* **2023**, *10*, 1270490. doi: 10.3389/fmars.2023.1270490
58. Pendleton, E.A., Thieler, E.R., Williams, S.J., Beavers, R.L. Coastal vulnerability assessment of Padre Island National Seashore (PAIS) to sea-level rise (No. 2004-1090). US Geological Survey. 2004.
59. Pereira, L.C.C., Silva, N.I.S., Costa, R.M., Asp, N.E., Costa, K.G., Vila-Concejo, A. Seasonal changes in oceanographic processes at an equatorial macrotidal beach in northern Brazil. *Cont Shelf Res* **2012**, *43*, 95–106. doi: 10.1016/j.csr.2012.05.003.
60. Oliveira, S., Moura, D., Horta, J., Nascimento, A., Gomes, A., Veiga-Pires, C. The morphosedimentary behaviour of a headland–beach system: Quantifying sediment transport using fluorescent tracers. *Mar Geol* **2017**, *388*, 62-73. DOI:10.1016/J.MARGEO.2017.02.010
61. Pessoa, R.M.C., Pereira, L.C.C., Sousa, R. C., Costa, R.A.M. Water Quality during the Recreational High Season for a Macrotidal Beach (Ajuruteua, Pará, Brazil). *J Coast Res* **2016**, *75*, 1222-1226. https://doi.org/10.2112/SI75-245.1
62. Pessoa, R.M.C., Jiménez, J.A., Costa, R.M., Pereira, L.C.C. Federal conservation units in the Brazilian amazon coastal zone: An adequate approach to control recreational activities? *Ocean Coast Manag* **2019**, *178*, 104856. https://doi.org/10.1016/j.ocecoaman.2019.104856
63. Pereira, L.C.C., Pessoa, R.M.C., Sousa-Felix, R.C., Dias, A.B.B., Costa, R.M. How sustainable are recreational practices on Brazilian Amazon beaches?. *J Outdoor Recreat Tour* **2024**, *45*, 100741. https://doi.org/10.1016/j.jort.2024.100741
64. Sousa, R.C., Pereira, L.C.C., Silva, N.I.S., Oliveira, S.M.O., Pinto, K.S.T., Costa, R.M. Recreational carrying capacity of three Amazon macrotidal beaches during the peak vacation season. *J Coastal Res* **2011**, *64*, 1292–1296. https://www.jstor.org/stable/26482383
65. Sousa, P.H., Siegle, E., Tessler, M.G. Vulnerability assessment of Massaguaçú beach (SE Brazil). *Ocean Coast Manag* **2013**, *77*, 24-30. https://doi.org/10.1016/j.ocecoaman.2012